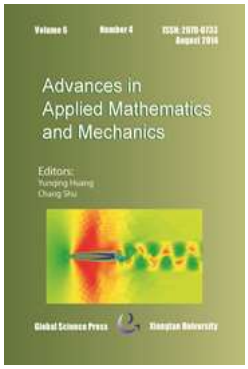

A Comparison and Unification of Ellipsoidal Statistical and Shakhov BGK Models

Songze Chen, Kun Xu and Qingdong Cai

Advances in Applied Mathematics and Mechanics / Volume 7 / Issue 02 / April 2015, pp 245 - 266
DOI: 10.4208/aamm.2014.m559, Published online: 10 March 2015

Link to this article: http://journals.cambridge.org/abstract_S2070073315000089

How to cite this article:
Songze Chen, Kun Xu and Qingdong Cai (2015). A Comparison and Unification of Ellipsoidal Statistical and Shakhov BGK Models. Advances in Applied Mathematics and Mechanics, 7, pp 245-266 doi:10.4208/aamm.2014.m559

Advances in Applied Mathematics and Mechanics
Adv. Appl. Math. Mech., Vol. **7**, No. 2, pp. 245-266

DOI: 10.4208/aamm.2014.m559
April 2015

A Comparison and Unification of Ellipsoidal Statistical and Shakhov BGK Models

Songze Chen[1], Kun Xu[1,2,*] and Qingdong Cai[2]

[1] *Hong Kong University of Science and Technology, Clear Water Bay, Kowloon, Hong Kong*
[2] *LTCS and CAPT, Department of Mechanics and Aerospace Engineering, College of Engineering, Peking University, Beijing 100871, China*

Received 30 March 2014; Accepted (in revised version) 26 August 2014

Abstract. The Ellipsoidal Statistical model (ES-model) and the Shakhov model (S-model) were constructed to correct the Prandtl number of the original BGK model through the modification of stress and heat flux. With the introduction of a new parameter to combine the ES-model and S-model, a generalized kinetic model can be developed. This new model can give the correct Navier-Stokes equations in the continuum flow regime. Through the adjustment of the new parameter, it provides abundant dynamic effect beyond the ES-model and S-model. Changing the free parameter, the physical performance of the new model has been tested numerically. The unified gas kinetic scheme (UGKS) is employed for the study of the new model. In transition flow regime, many physical problems, i.e., the shock structure and micro-flows, have been studied using the generalized model. With a careful choice of the free parameter, good results can be achieved for most test cases. Due to the property of the Boltzmann collision integral, the new parameter in the generalized kinetic model cannot be fully determined. It depends on the specific problem. Generally speaking, the S-model predicts more accurate numerical solutions in most test cases presented in this paper than the ES-model, while ES-model performs better in the cases where the flow is mostly driven by temperature gradient, such as a channel flow with large boundary temperature variation at high Knudsen number.

AMS subject classifications: 65M10, 78A48

Key words: Kinetic models, unified gas kinetic scheme, rarefied flow.

1 Introduction

The monatomic rarefied gas behavior can be described by the Boltzmann equation. However, the collision term of the Boltzmann equation is a multiple integral term which is

*Corresponding author.
Email: jacksongze@pku.edu.cn (S. Z. Chen), makxu@ust.hk (K. Xu), caiqd@pku.edu.cn (Q. D. Cai)

very complicated for analysis and numerical computation. Bhatnagar et al. [1] simplified the collision term in the Boltzmann equation and proposed BGK model in which the Boltzmann collision term is replaced by a relaxation term. This relaxation term mimics the main relaxation process from nonequilibrium state towards to a local equilibrium one. The local equilibrium state known as Maxwell distribution function is determined by the local conservative flow variables, namely, the mass, momentum and energy. Due to its simplicity, the BGK model becomes an important kinetic model for analysis and numerical simulation of nonequilibrium flows. However, the Chapman-Enskog expansion of the BGK model derives the Navier-Stokes equations with a unit Prandtl number, which is different from the physical reality in the continuum flow regime. For a monatomic gas, the accepted Prandtl number is about 2/3 in a wide range of flow conditions.

In order to fix the Prandtl number, many kinetic models have been proposed in the past decades. The main approach is to modify the relaxation term. For example, the Ellipsoidal Statistical BGK model [2] employs a Gaussian distribution as the relaxation equilibrium state instead of the Maxwell distribution. This model is not very popular until Andries [3] proved the entropy condition of the ES-model. In the ES-model, besides the conservative flow variables, the local stress tensor also involves in the relaxation term. By changing the free parameter in the ES-model, it can present an arbitrary Prandtl number. Moreover, the nonnegative property of the Gaussian distribution is a favorable physical property.

Another very popular kinetic model is the Shakhov model [4]. Unlike the ES-model, it adjusts the heat flux in the relaxation term. With the implementation of Hermite polynomial, the low order moments of relaxation term in S-model are identical to the original BGK one, namely, the conservative variables are maintained and the stress tensor keeps isotropic one as that from the BGK model. Only the third order moments of relaxation term change. In other words, the S-model modifies the BGK model by adjusting heat flux to present the correct Prandtl number. But, it allows negative value of distribution function and its H-theorem was only proved in near equilibrium condition [4].

In 1990, Liu [5] proposed a new kinetic model by considering the gain term and lost term of the Boltzmann equation separately, where the Chapman-Enskog distribution is directly used to evaluate the relaxation term. Therefore, the space derivatives are involved in the collision term. Liu model changes both the heat flux and stress tensor of the relaxation process and provides a correct Prandtl number in the continuum flow regime. Due to its relatively complicated formulation, this model has not been widely used.

Although all above models provide correct Prandtl number in the continuum flow regime, their properties are very different in the transition regime [6–10]. Garzo [7] reported a singular behavior of Liu model and attributed it to the negative distribution function. Graur [8] studied the heat transfer problem and found that the ES-model provides better results than the S-model through the comparison with the results from the Boltzmann equation. The ES-model keeps the distribution function positive, while the S-model and Liu model always allow un-physical negative distribution function. It seems

that the nonnegative properties of the ES-model are important and promising. Moreover, the ES-model satisfies the H theorem, while the H-theorem of the S-model is only proved in the near local equilibrium state [9]. However, some other studies did not tell the same story. Mieussens [11] and Kudryavtsev [10] both reported the early rising of temperature profile in the shock structure solution derived by the ES-model.

In fact, the physical performance of these models has not yet been evaluated extensively in the transition regime. The properties, such as the H-theorem, nonnegative distribution and conservation etc., cannot cover a complete physical picture of dynamics of the particle collision term and the evolution of the distribution function. The original motivation for the development of the kinetic models is to fix the Prandtl number which is well defined in the continuum flow regime. In transition regime, it is expected that significant differences in their performance would appear in different physical problems. Furthermore, the practical applications care more about the macroscopic quantities, such as the moments of a distribution function. The H-theorem and the nonnegative distribution function only present a portion of physical conditions, but is not sufficient to guarantee a correct dynamic evolution of macroscopic quantities. So, it is necessary to inspect the practical performance of different kinetic models through the numerical simulations in the transition regime. In order to cover a whole range of dynamic performance of kinetic models, we are going to introduce a generalized kinetic model which combines the ES-model and S-model. With the combination of these two models, besides obtaining the correct Prandtl number, we have one more free parameter to be adjusted. With the variation of this parameter, a continuum dynamic performance from the ES-model to the S-model and beyond, can be identified.

In the past years, a unified gas kinetic scheme (UGKS) [12–16] has been well developed. The BGK model and the S-model have been employed in the UGKS. In this paper we will use the UGKS framework to construct numerical scheme for the generalized kinetic model. The numerical scheme will be used to examine physical performance of different kinetic models with the variation of the parameter, where both the ES-model and the S-model become limiting cases. A continuous dynamic transition between these two models can be obtained. Through investigations, the performances of different kinetic models under different flow conditions in the transition regime are presented in details.

This paper is organized as follows. Section 2 introduces criteria for the construction of kinetic model. Section 3 proposes a generalized kinetic model. Section 4 gives the simulation results of the new model in the shock structure and microflow computations. The parameter dependent dynamic effect will be discussed in different test cases. Section 5 presents the analysis and insight of the new model. The last section is the conclusion.

2 Criteria for the construction of kinetic models

The Boltzamnn equation formally reads as follows,

$$f_t+\mathbf{u}\cdot\nabla f=\mathcal{J}(f), \tag{2.1}$$

where $\mathcal{J}(f)$ denotes the collision term. Here f represents the velocity distribution function which is a function of the physical space location $\mathbf{x}$ and the molecule velocity $\mathbf{u}$. The macroscopic quantities, such as, the mass ρ, momentum $\rho\mathbf{U}$ (ρU_i), energy ρE, stress tensor $\mathbf{P}$ (P_{ij}) and heat flux $\mathbf{q}$ (q_i), can be derived from the distribution function f,

$$W=\begin{pmatrix}\rho\\ \rho\mathbf{U}\\ \rho E\end{pmatrix}=\int\psi f d\mathbf{u}, \tag{2.2a}$$

$$P_{ij}=\int(u_i-U_i)(u_j-U_j)f d\mathbf{u}, \tag{2.2b}$$

$$q_i=\int\frac{1}{2}(u_i-U_i)(\mathbf{u}-\mathbf{U})^2 f d\mathbf{u}, \tag{2.2c}$$

where ψ is defined as follows,

$$\psi=\left(1,\mathbf{u},\frac{1}{2}\mathbf{u}^2\right)^T, \tag{2.3}$$

and $d\mathbf{u}$ is the volume element in the velocity space. Since the mass, momentum and energy are conserved during particle collisions, the collision term satisfies the conservation constraint,

$$\int\mathcal{J}(f)\psi d\mathbf{u}=\mathbf{0}, \tag{2.4}$$

at any location and any time.

Taking moments of Eq. (2.1), the corresponding macroscopic equations [17,18] read,

$$\rho_t+\nabla\cdot(\rho\mathbf{U})=0, \tag{2.5a}$$

$$(\rho\mathbf{U})_t+\nabla\cdot(\rho\mathbf{U}\mathbf{U}+p\mathbf{I})+\nabla\cdot\mathbf{p}=0, \tag{2.5b}$$

$$(\rho E)_t+\nabla\cdot((\rho E+p)\mathbf{U})+\nabla\cdot(\mathbf{q}+\mathbf{p}\cdot\mathbf{U})=0, \tag{2.5c}$$

$$(\mathbf{P})_t+\nabla\cdot\int(\mathbf{u}-\mathbf{U})(\mathbf{u}-\mathbf{U})(\mathbf{u}-\mathbf{U})f d\mathbf{u}=\mathbf{S_p}, \tag{2.5d}$$

$$(\mathbf{q})_t+\nabla\cdot\int\frac{1}{2}(\mathbf{u}-\mathbf{U})(\mathbf{u}-\mathbf{U})(\mathbf{u}-\mathbf{U})^2 f d\mathbf{u}=\mathbf{S_q}, \tag{2.5e}$$

where p denotes the pressure defined as $p=\text{trace}(\mathbf{P})/3$ and shear stress is defined as $\mathbf{p}=\mathbf{P}-p\mathbf{I}$. The source terms read as follows,

$$\mathbf{S_p}=\int(\mathbf{u}-\mathbf{U})(\mathbf{u}-\mathbf{U})\mathcal{J}(f)d\mathbf{u}, \tag{2.6a}$$

$$\mathbf{S_q}=\int\frac{1}{2}(\mathbf{u}-\mathbf{U})(\mathbf{u}-\mathbf{U})^2\mathcal{J}(f)d\mathbf{u}. \tag{2.6b}$$

This set of macroscopic equations is identical for different collision terms or kinetic models due to the conservative property of the particle collision term.

Generally, a kinetic model takes the following formulation,

$$\frac{\partial f}{\partial t}+\mathbf{u}\cdot\frac{\partial f}{\partial\mathbf{x}}=\mathcal{J}'(f)=\frac{g^+-f}{\tau}, \tag{2.7}$$

where g^+ is the post collision term and τ denotes the relaxation time. The purpose of constructing kinetic model is to get physical insight of rarefied gas system and capture the flow behavior with minimum mathematical complexity. In the modeling process, certain information about the gas system, such as the individual particle collision trajectory, has to be ignored. But, the recovered macroscopic equations should be maintained as precisely as possible in comparison with the corresponding ones of the Boltzmann equation. The moment equations are accurate in all flow regimes if the last two equation of Eq. (2.5) is accurate. In fact, from the view of macroscopic quantities, the different gas molecules or kinetic models are reflected in two parts, one is the source terms $\mathbf{S}_p$ and $\mathbf{S}_q$, and the other is convection term in the last two equations of Eq. (2.5) which induce the closure problem. In this study, we focus on the first one, the source terms, which represent the relaxation processes of stress and heat flux. Different relaxation processes of the kinetic models are compared with that of the Boltzmann solution.

3 A generalized kinetic model

As we know, the ES-model and S-model change either the stress tensor or the heat flux of the post collision terms to achieve a correct Prandtl number. It is quite straightforward to combine these two approaches together. It's obvious that this kind of modification could also give a correct Prandtl number and provide a free parameter as a by-product.

For the ES-model, g^+ is written as

$$g^+ = \mathcal{G}[f] = \frac{\rho}{\sqrt{\det(2\pi\mathbf{T})}} \exp\Big(-\frac{1}{2}\mathbf{c}\cdot\mathbf{T}^{-1}\cdot\mathbf{c}\Big). \tag{3.1}$$

Here, $\mathbf{T}$ is a tensor related to the stress tensor $\mathbf{P}$,

$$\mathbf{T} = (1-C_{es})RT\mathbf{I} + C_{es}\mathbf{P}/\rho, \tag{3.2}$$

where R is gas constant, T is gas temperature and $\mathbf{c} = \mathbf{u} - \mathbf{U}$ is peculiar velocity. In the Shakhov model, g^+ takes the form,

$$g^+ = \mathcal{M}[f] + \mathcal{S}[f], \tag{3.3a}$$

$$\mathcal{S}[f] = \mathcal{M}[f]\Big[(1-C_{shak})\mathbf{c}\cdot\mathbf{q}\Big(\frac{c^2}{RT}-5\Big)\Big/(5pRT)\Big], \tag{3.3b}$$

$$\mathcal{M}[f] = \frac{\rho}{\sqrt{\det(2\pi RT\mathbf{I})}} \exp\Big(-\frac{1}{2RT}\mathbf{c}^2\Big), \tag{3.3c}$$

where $\mathcal{M}[f]$ denotes the Maxwell distribution function. and C_{shak} is a parameter which is related to the Prandtl number in this model.

Replacing the Maxwell distribution by the Gaussian distribution in the S-model, the post collision term of the generalized kinetic model is

$$g^+ = \mathcal{G}[f] + \mathcal{S}[f]. \tag{3.4}$$

The two coefficients, C_{es} and C_{shak}, are two independent parameters at this moment. In order to obtain the right transport coefficients, we follow the proof of Andries [3]. In continuum regime, the distribution function is expanded as,

$$f=\mathcal{G}[f]+\mathcal{S}[f]-\tau(\mathcal{M}_t+\mathbf{u}\cdot\mathcal{M}_{\mathbf{x}})+o(\tau). \tag{3.5}$$

For stress tensor, the above distribution function gives,

$$\mathbf{P}=(1-C_{es})\rho RT\mathbf{I}+C_{es}\mathbf{P}+\mathbf{p}_{bgk}, \tag{3.6}$$

then

$$\mathbf{p}=\frac{1}{(1-C_{es})}\mathbf{p}_{bgk}. \tag{3.7}$$

And heat flux is,

$$\mathbf{q}=(1-C_{shak})\mathbf{q}+\mathbf{q}_{bgk}, \tag{3.8}$$

then

$$\mathbf{q}=\frac{1}{C_{shak}}\mathbf{q}_{bgk}. \tag{3.9}$$

As a result, the Prandtl number for the generalized kinetic model is

$$\mathrm{Pr}=\frac{C_{shak}}{1-C_{es}}\mathrm{Pr}_{bgk}=\frac{C_{shak}}{1-C_{es}}. \tag{3.10}$$

And the viscosity from the distribution function (Eq. (3.5)) is

$$\mu=\frac{\tau p}{1-C_{es}}. \tag{3.11}$$

Considering a spatially homogenous monatomic gas, the following three moment equations can be obtained from the generalized model,

$$\frac{\partial f}{\partial t}=-\frac{1}{\tau}(f-g^{+}),\quad \frac{\partial \mathbf{P}}{\partial t}=\frac{\partial \mathbf{p}}{\partial t}=\frac{-(1-C_{es})}{\tau}\mathbf{p},\quad \frac{\partial \mathbf{q}}{\partial t}=\frac{-C_{shak}}{\tau}\mathbf{q}, \tag{3.12}$$

present three different relaxation processes, namely, the relaxation of distribution function itself, the relaxation of second order moments and the relaxation of third order moments. The ratios between different relaxation rates are determined by the two coefficients, C_{es} and C_{shak}.

If Prandtl number is fixed, there is only one free parameter in the generalized model. Here, the C_{es} is taken as a free parameter. When $C_{es}=0$ and $C_{shak}=\mathrm{Pr}$, the generalized model is identical to the Shakhov model. When $C_{es}=1-1/\mathrm{Pr}$ and $C_{shak}=1$, it gives the ES-model. When $C_{es}=0$ and $C_{shak}=1$, it presents the BGK model. And for the other values, the generalized kinetic model shows how the ES-model changes to the Shakhov model continuously. And the new free parameter might provide an opportunity to preserve additional physical properties in the full Boltzmann collision term.

4 Numerical results

In this section, the generalized kinetic model is solved by the unified gas kinetic scheme (UGKS) [12–16]. At first, we will briefly introduce the UGKS.

4.1 Unified gas kinetic scheme for kinetic models

The unified gas kinetic scheme is a direct modeling method to simulate gas flow in the whole Knudsen number regimes. It is a finite volume conservation law for the evolution of gas distribution function.

Taking the collision time as a local constant, there is an analytic solution for kinetic model (Eq. (2.7)),

$$f(\mathbf{x},t,\mathbf{u})=e^{-t/\tau}f_0(\mathbf{x}-\mathbf{u}t)+\frac{1}{\tau}\int_0^t g^+(\mathbf{x}',t',\mathbf{u})e^{-(t-t')/\tau}dt', \tag{4.1}$$

where $\mathbf{x}'=\mathbf{x}-\mathbf{u}(t-t')$.

Applying this solution at cell interface, the mass flux, momentum flux and energy flux can be obtained as follows,

$$\mathcal{F}_{macro}=\begin{pmatrix}\mathcal{F}_{mass}\\ \mathcal{F}_{momentum}\\ \mathcal{F}_{energy}\end{pmatrix}=\begin{pmatrix}\mathbf{n}\cdot\int_{\Omega_\mathbf{u}}\mathbf{u}f d\mathbf{u}\\ \mathbf{n}\cdot\int_{\Omega_\mathbf{u}}\mathbf{u}\mathbf{u}f d\mathbf{u}\\ \mathbf{n}\cdot\int_{\Omega_\mathbf{u}}\mathbf{u}\frac{1}{2}\mathbf{u}^2 f d\mathbf{u}\end{pmatrix}. \tag{4.2}$$

The $\Omega_\mathbf{u}$ denotes the entire velocity space and $\mathbf{n}$ is the normal direction of the cell interface.

The flux of velocity distribution function at particle velocity $\mathbf{u}_k$ takes the following form:

$$\mathcal{F}_{\mathbf{u}_k}=\mathbf{n}\cdot\int_{\Omega_{\mathbf{u}_k}}\mathbf{u}f d\mathbf{u}, \tag{4.3}$$

where $\Omega_{\mathbf{u}_k}$ denotes the velocity space around $\mathbf{u}_k$.

Applying the conservation law, the evolution of flow quantities can be obtained. Owing to the absence of source term, the evolution of the macroscopic conservative quantities becomes,

$$W^{n+1}=W^n-\frac{1}{V_{\mathbf{x}_i}}\int_{t^n}^{t^{n+1}}\sum_m \Delta S_m\mathcal{F}_{macro}dt, \tag{4.4}$$

where $V_{\mathbf{x}_i}$ is the volume of $\Omega_{\mathbf{x}_i}$ in the physical space, ΔS_m is the area of interface and m is the index of surfaces of $\Omega_{\mathbf{x}_i}$. The collision term must be considered for the update of the

distribution function. Here, we use two steps to update the distribution function

$$f^{*}_{\mathbf{u}_k} = f^{n}_{\mathbf{u}_k} - \frac{1}{V_{\mathbf{x}_i}} \int_{t^n}^{t^{n+1}} \sum_m \Delta S_m \mathcal{F}_{\mathbf{u}_k} + \Delta t \frac{g^{+(n)}_{\mathbf{u}_k} - f^{n}_{\mathbf{u}_k}}{\tau^n}, \tag{4.5a}$$

$$f^{n+1}_{\mathbf{u}_k} = f^{n}_{\mathbf{u}_k} - \frac{1}{V_{\mathbf{x}_i}} \int_{t^n}^{t^{n+1}} \sum_m \Delta S_m \mathcal{F}_{\mathbf{u}_k} + \frac{\Delta t}{2}\Big(\frac{g^{+(*)}_{\mathbf{u}_k} - f^{n+1}_{\mathbf{u}_k}}{\tau^{n+1}} + \frac{g^{+(n)}_{\mathbf{u}_k} - f^{n}_{\mathbf{u}_k}}{\tau^n}\Big), \tag{4.5b}$$

$$\begin{aligned} f^{n+1}_{\mathbf{u}_k} = {} & \frac{\Delta t}{2\tau^{n+1}+\Delta t} g^{+(*)}_{\mathbf{u}_k} + \frac{\tau^{n+1}}{\tau^n}\frac{\Delta t}{2\tau^{n+1}+\Delta t} g^{+(n)}_{\mathbf{u}_k} + \frac{2\tau^n - \Delta t}{2\tau^{n+1}+\Delta t} f^{n}_{\mathbf{u}_k} \\ & - \frac{2\tau^{n+1}}{2\tau^{n+1}+\Delta t}\frac{1}{V_{\mathbf{x}_i}} \int_{t^n}^{t^{n+1}} \sum_m \Delta S_m \mathcal{F}_{\mathbf{u}_k}. \end{aligned} \tag{4.5c}$$

A medium state f^{*} is estimated first. Then solve the second equation and get $f^{n+1}_{\mathbf{u}_k}$ at the next time level. The above procedure is identical for an arbitrary g^{+}. For the details of the numerical reconstruction, please refer to the articles about gas kinetic scheme [12, 13, 19].

The UGKS is a direct physical modeling of flow motion in the scale of the discretized space and the integral solution (Eq. (4.1)) for the kinetic model covers the flow evolution from kinetic to the hydrodynamics scales. The specific flux used at the cell interface depends on the ratio of time step to the local particle collision time (see the term $e^{-t/\tau}$). Such unique merits enable the UGKS to recover correct fluxes in the whole Knudsen number ranges including free molecule regime, transition regime and continuum regime. In the following numerical simulations, the velocity space is uniformly discretized. And Newton-Cotes quadrature rules are adopted for the integration of velocity space. Without specification, the velocity points cover the velocity range of $[-(|U_{ref}|+4.5\sqrt{RT_{ref}}), |U_{ref}|+4.5\sqrt{RT_{ref}}]$.

4.2 Force driven Poiseuille flow

In the force driven Poiseuille flow, the external force drives the flow motion between two fixed plates. The flow field will achieve a steady state when the external force is balanced by the shear stress from the fixed boundaries. We consider monatomic gas in this simulation. To follow the study [20], the Knudsen number is defined as,

$$\mathrm{Kn} = \sqrt{\frac{\pi}{2}}\frac{\mu_0\sqrt{RT_0}}{p_0 L}, \tag{4.6}$$

where L is the width of the channel and subscript 0 denotes the initial value of variables. The gas is confined between two vertical plates which locate at $x=-0.5$ and $x=0.5$ respectively. The temperature of the plates is $T_w=1$. The initial flow states are shown as follows, $T_0=1$, $\rho_0=1$, $p_0=1$. The gravity is represented by G and is upward in the vertical direction. Here the hard sphere molecule is adopted, namely, the viscosity-temperature

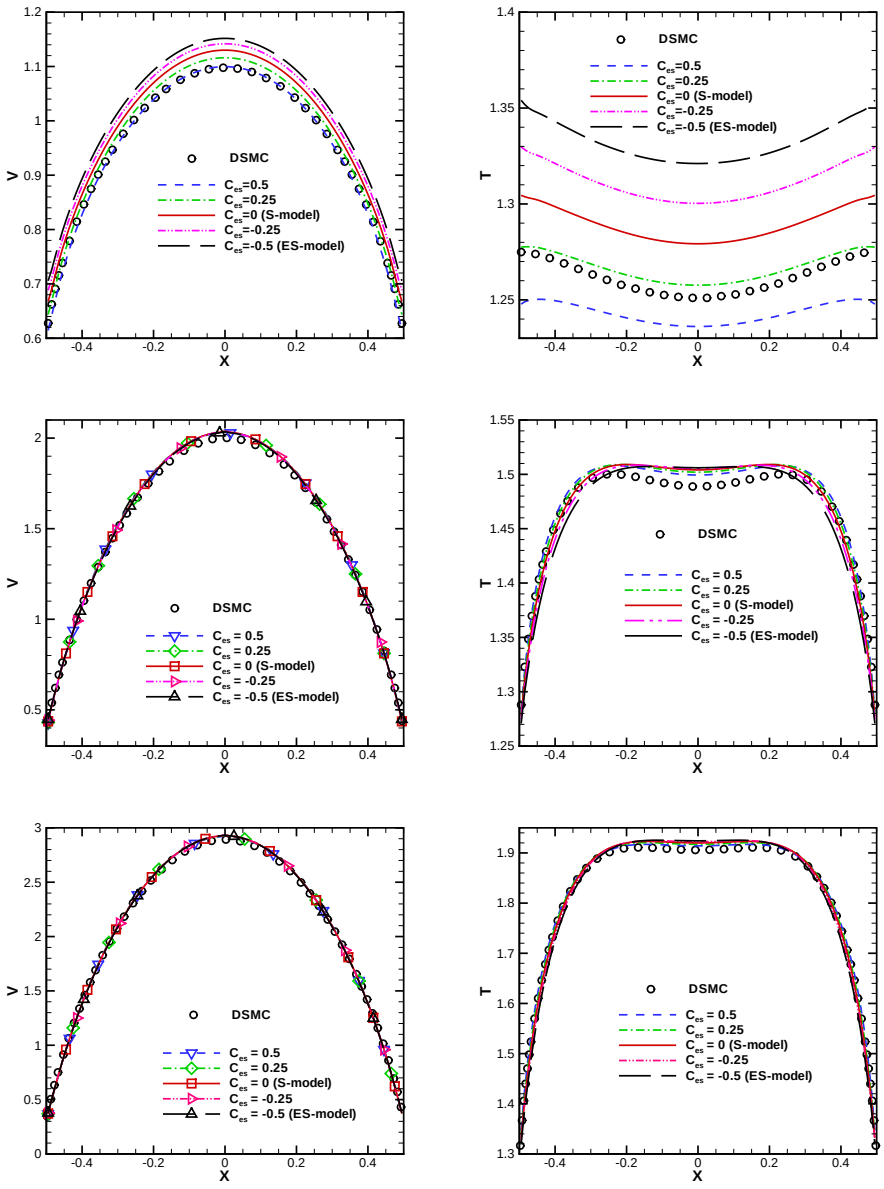

Figure 1: The velocity and temperature profiles for force driven Poiseuille flow derived from the generalized kinetic model under different Knudsen numbers. The Knudsen numbers are 1, 0.1 and 0.05 respectively from top to bottom. And the Gravity is $G=1$.

coefficient is $\omega=0.5$, i.e., $\mu\sim T^{\omega}$. The gas-wall interaction is fully diffusive kinetic boundary condition. Due to the unreasonable large value of $G=1$, this test becomes a very difficult simulation and the distribution function is totally distorted by the external force, especially at high Knudsen number. Therefore, the discrete velocity point must extend to very far place and be modified manually in the force direction. The upper bound of

vertical velocity extends to $8\sqrt{RT_0}$. Here C_{es} varies from -0.5 to 0.5 in the generalized kinetic model. The two special cases, the ES-model and the S-model, are included in this set of simulations.

As shown in Fig. 1, when the Knudsen number is small, say, Kn $= 0.05$, the difference between results from different kinetic models and the DSMC is small. But, as the Knudsen number becomes large, the temperature profiles separate from each other. For all Knudsen numbers, the results from the S-model are closer to the DSMC results than that from the ES-model. The profiles with different C_{es} cover the results of ES-model and S-model. And when the C_{es} is larger than 0, the temperature profile moves from the S-model result to the DSMC result. It is clearly shown that the generalized kinetic model can predict more accurate results in comparison with the S-model and ES-model if C_{es} is specified properly.

4.3 Couette flow

In this case, we also consider the monatomic gas between two plates. The left and right plates move with the same speed (300), but with opposite directions. The left one moves downward and the right one moves upward. The temperatures of gas and plates both are 273. The reference viscosity is defined as,

$$\mu_{ref} = \frac{30}{(7-2\omega)(5-2\omega)} \frac{\rho\lambda\sqrt{2\pi RT}}{4}. \tag{4.7}$$

The viscosity-temperature coefficient ω is 0.81. The solutions are compared with the DSMC results [21]. The Prandtl number is 2/3. In current simulation, the spatial coordinate is ranged from -50 to 50 and is discretized with 100 cells. The Knudsen number is varied by the changing of gas density.

Fig. 2 shows the velocity and temperature profiles from the different kinetic models. When Knudsen number is 0.01, the results from different kinetic models are almost identical with the DSMC results. While Knudsen number becomes large, the velocity and temperature profiles separate gradually. The cases in which $C_{es} = 0$ or 0.25 present most satisfactory results compared with the DSMC results, especially for Kn $= 0.1$. When Knudsen number is 1, the temperature profiles move away from the DSMC results. Based on these numerical data, we show that the generalized kinetic model with different parameters present the same continuum limit when Knudsen number is small. In the medium Knudsen number regime, the S-model perform the best. For low speed Couette flow, we consider the case presented in [22]. Hard sphere model is adopted. The initial value is 1 for the density and temperature. The wall speed is only ± 0.2. The Knudsen number is defined by Eq. (4.6). Since the velocity profiles are very close to each other, we only present temperature profiles. As shown in Fig. 3, the generalized kinetic model with $C_{es} = 0.25$ gives the best results.

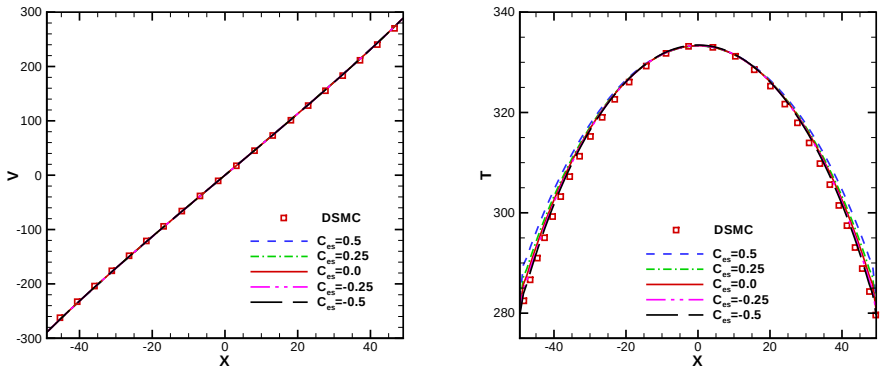

(a) $Kn = 0.01$

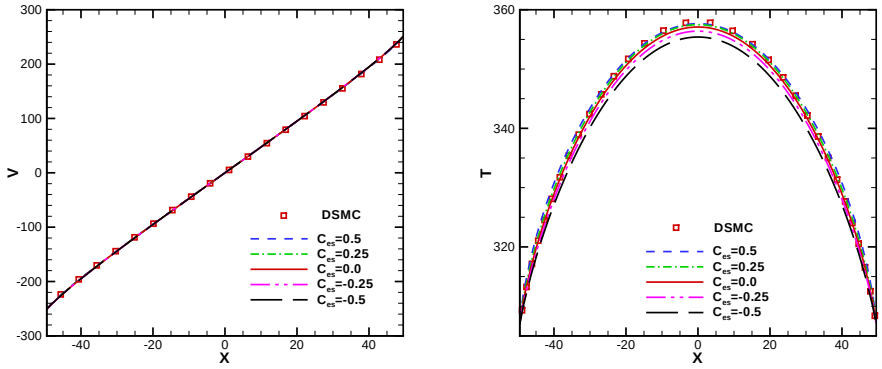

(b) $Kn = 0.1$

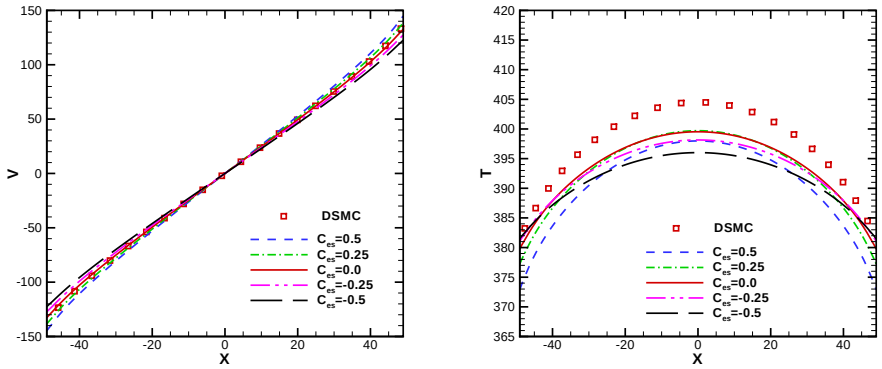

(c) $Kn = 1$

Figure 2: The velocity and temperature profiles for Couette flow problem.

4.4 Unsteady boundary heating

The numerical configuration is identical to the unsteady boundary heating problem in the study [22]. The gas is heated by two walls with time-dependent temperatures $T_w =$

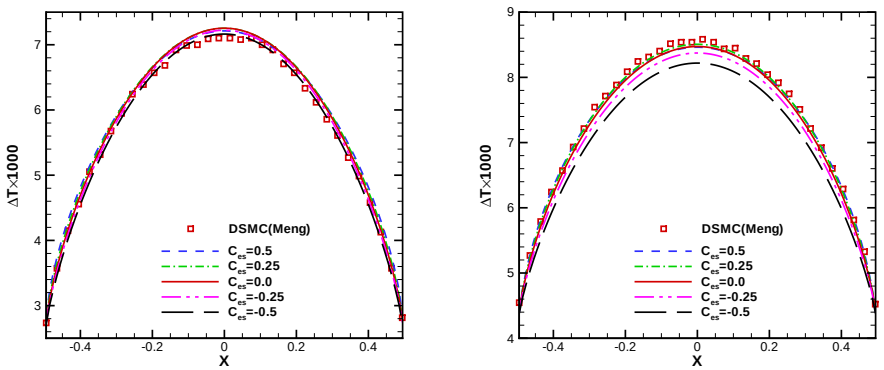

(a) $Kn=0.1$ (b) $Kn=0.2$

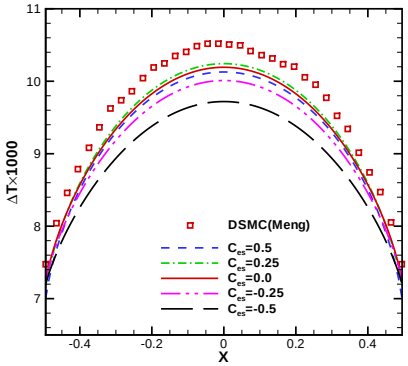

(c) $Kn=0.5$

Figure 3: The temperature profiles $(\Delta T=T-T_0)$ for low speed Couette flow problem. The DSMC results are extracted from the reference [22].

$T_0(1+0.002\sin(\theta t))$, $T_0=1$. Hard sphere molecule is adopted in the simulation. And the Prandtl number is $2/3$. The Knudsen number is defined as follows,

$$\mathrm{Kn}=\frac{16}{5\sqrt{2\pi}}\frac{\mu_0\sqrt{RT_0}}{p_0L}. \tag{4.8}$$

Fig. 4 presents the velocity and temperature profiles at $\theta t=3\pi/2$. The U velocity is normalized by 2×10^{-5} and ΔT is defined as $\Delta T=(T-T_0)/(0.002T_0)$. Obviously, the results from the S-model is closer to the LVDSMC [23] results. When C_{es} is larger than 0, the generalized kinetic model gives a better result. The corresponding coefficient is very close to the one in the force driven Poiseuille flow.

4.5 Response of a gas to a spatially varying boundary temperature

This simulation is about the response of a gas to a spatially varying boundary temperature in 2-D domain. The numerical setup is the same as the study [24]. Gas is confined

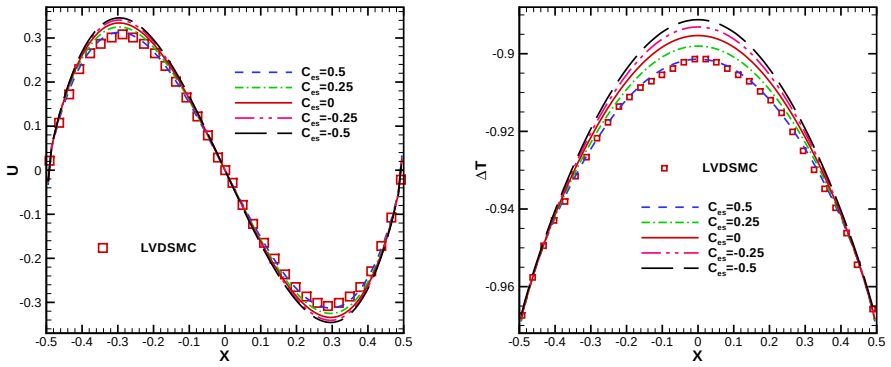

(a) Kn = 0.1, $\theta = \phi$

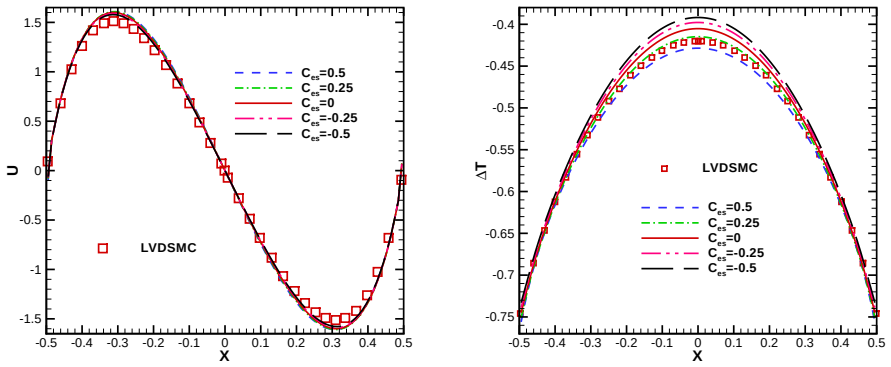

(b) Kn = 0.2, $\theta = 4\phi$

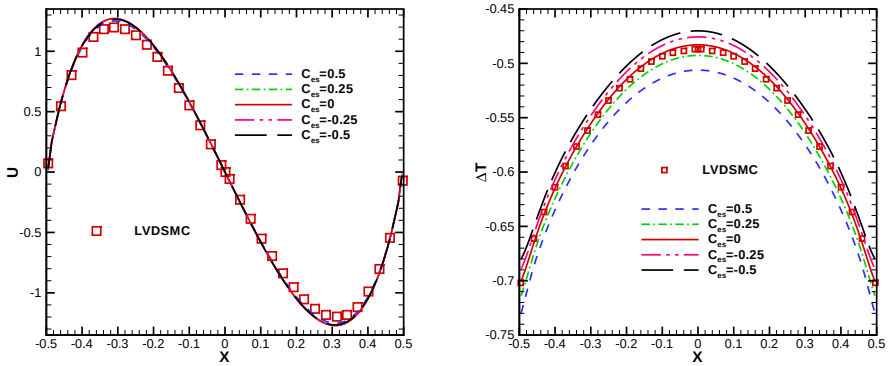

(c) Kn = 0.5, $\theta = 4\phi$

Figure 4: The velocity and temperature profiles for unsteady boundary heating problem at $\theta t = 3\pi/2$. The ϕ is defined as $\phi = \pi\sqrt{2}/16$.

between two horizontal boundaries. The lower boundary at $y = 0$ is fully diffusive with a temperature given by $T_w = T_0(1 - 0.5\cos(2\pi x))$. An identical boundary is located at $y = 1$.

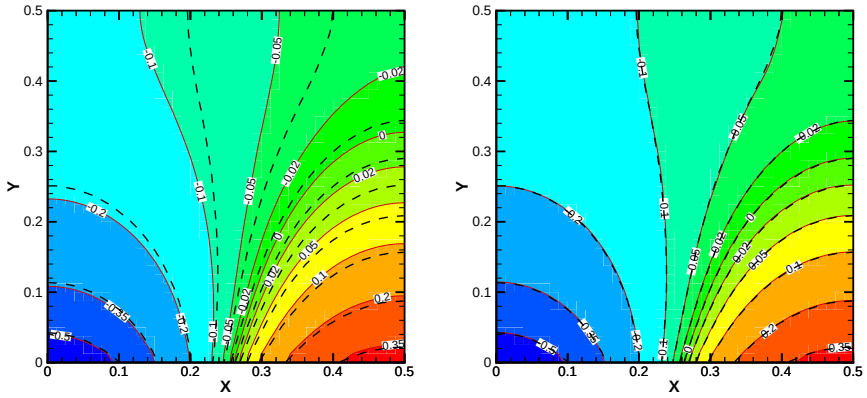

Figure 5: The temperature deviation contour of a spatially boundary temperature variation problem. The dash line is DSMC data extracted from the reference [24].

The Knudsen number based on the separation between the two boundaries is 1. Working gas is argon with reference viscosity defined by Eq. (4.7). Owing to the symmetries in the x and y directions, the simulation domain is chosen as $[0,1/2]\times[0,1/2]$. Fig. 5 shows the temperature deviation contours derived from ES-model and S-model. The temperature deviation is defined as $\Delta T=(T-T_0)/0.5$. The background data is extracted from the reference [24]. Unlike the previous two test cases, ES-model predicts more accurate results than the S-model does in comparison with DSMC results.

4.6 Shock structure

The shock structure is a typical example of non-equilibrium flow structure and is a distinguishable test case. Kinetic models show very different performances in shock structure simulation. To examine capabilities of the ES-model and the S-model, Mach 8 argon shock structure is simulated and the solutions are compared with the DSMC results [21]. The DSMC code is provided by G. A. Bird. The viscosity-temperature coefficient ω is 0.81. The Prandtl number is $2/3$. And the reference viscosity is defined by Eq. (4.7). In current simulation, the spatial coordinate is normalized by the upstream mean free path, namely, the upstream mean free path of argon is 1. The computational spatial domain is $[-50,30]$ and is uniform meshed by 300 points. The quantities W are normalized as $\widetilde{W}=(W-W_1)/(W_2-W_1)$, where the subscript 1 denotes upstream quantity and 2 denotes downstream quantity.

Fig. 6 gives the density and temperature profiles from the ES-model and S-model. The S-model and the DSMC present almost identical density profiles. But the temperature rises a little bit early for the S-model. In comparison with the S-model, the ES-model predicts a narrow density profile and a wide temperature profile. Obviously, the S-model performs much better than ES-model in shock structure calculations.

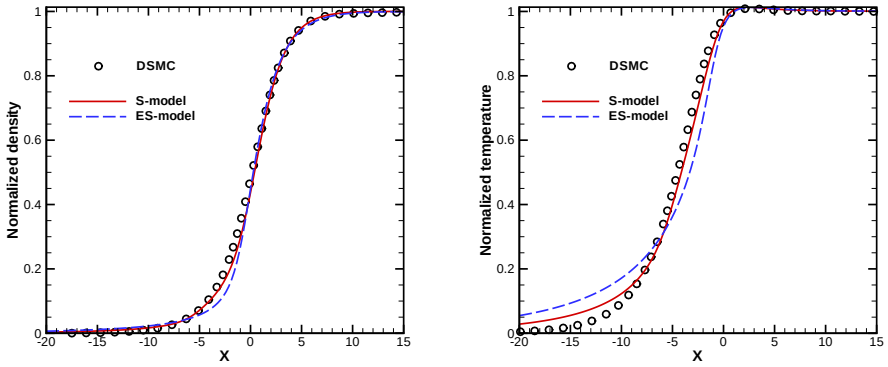

Figure 6: The shock structure for ES-model and S-model at Ma $=8$ and $\omega=0.81$.

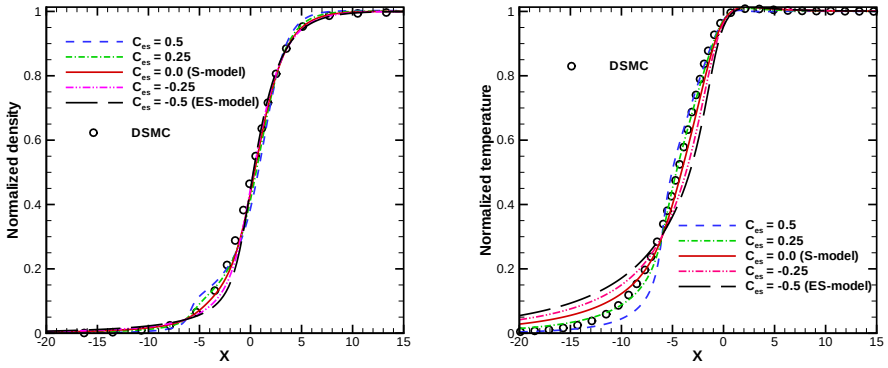

Figure 7: The shock structure for the generalized kinetic model with different C_{es} at Ma $=8$ and $\omega=0.81$.

Fig. 7 shows the tendency how the shock structure changes while the C_{es} varies from -0.5 to 0.5. Note that Pr $=2/3$ is fixed in all these results. The generalized kinetic model presents a set of shock structures with the same Prandtl number. When the $C_{es}=-0.5$, the generalized kinetic model presents the ES-model. As the value of C_{es} becomes larger, the temperature profile becomes steeper. Meanwhile, the density profile grows wider. When C_{es} is larger than 0, the temperature profile still becomes steepening. But when C_{es} exceeds 0.15, the density profile turns out to be twisted near the upstream. Although the annoyed twisting density profile makes this range of the free parameter unacceptable, the strong dependence of the C_{es} is confirmed.

5 Analysis

The individual ES-model and S-model were constructed to set the Prandtl number as a free parameter. Physically, the Prandtl number of a monatomic gas has a fixed value, especially in the continuum flow regime. Therefore, the Prandtl number should not be taken as a free parameter for monatomic ideal gas. With a fixed Prandtl number, theoret-

ically there is not any freedom in the ES-model and S-model. In this study we propose a generalized kinetic model. Besides a fixed Prandtl number for monatomic gas, the new model provides one more free parameter. This free parameter can present a continuum spectrum of kinetic models with a fixed Prandtl number. And it provides ways to mimic more complicated physical relaxation process. With certain choices of this free parameter, say C_{es}, the S-model and ES-model become a subset of the new model.

As mentioned in Section 3, C_{es} and C_{shak} are related to the relaxation of moments of the distribution function and they should behave similar to the counterpart from Boltzmann equation. To shed light on this topic, we examine the Boltzmann collision term for VHS molecule. The Boltzmann equation is written as following,

$$\frac{\partial(nf)}{\partial t}+\mathbf{u}\cdot\frac{\partial(nf)}{\partial \mathbf{x}}=\mathcal{J}(nf), \tag{5.1}$$

where f is normalized distribution function, n represents the particle number density and $\mathcal{J}(nf)$ denotes the Boltzmann collision term. The collision integral is defined as

$$\Delta[Q]=\int_{-\infty}^{+\infty}\int_{-\infty}^{+\infty}\int_{0}^{4\pi} n^2 Q(f^* f_1^* - f f_1) c_r \sigma d\Omega d\mathbf{u} d\mathbf{u_1}, \tag{5.2}$$

where Ω is the solid angle for scattering molecule, c_r is the relative velocity between two colliding molecules and σ is the collision cross section. For a spatially homogenous monatomic gas problem, the moments equation of the Boltzmann equation gives the relaxation process of the moments. For the quantity Q, the relaxation process can be written as

$$\frac{m\partial\langle nf,Q\rangle}{\partial t}=m\Delta[Q], \tag{5.3}$$

where $\langle nf,Q\rangle=\int nfQd\mathbf{u}$ and m is the mass of molecule. For example, if $Q=u^2$ and for Maxwell molecule, i.e., $\mu\sim T$, the corresponding relaxation equation is

$$\frac{\partial P_{11}}{\partial t}=\frac{\partial p_{11}}{\partial t}=m\Delta[u^2]. \tag{5.4}$$

The collision integral can be obtained explicitly for Maxwell molecule [21] and reads as following,

$$\frac{\partial p_{11}}{\partial t}=-\frac{p}{\mu}p_{11}. \tag{5.5}$$

For the other molecules, there is no explicit solution. However, some qualitative results can be deduced from a given distribution function. Here, we only consider two kinds of distribution functions for VHS molecule. The diameter of VHS molecule is given by

$$d=d_{ref}(c_{r,ref}/c_r)^v, \tag{5.6}$$

where $v=\omega-1/2$. The first distribution function is the one employed in Grad's thirteen moments method [25] and it reads

$$f=\mathcal{M}[f]\Big(1+\mathbf{c}\cdot\frac{\mathbf{P}-p\mathbf{I}}{2pRT}\cdot\mathbf{c}+\frac{\mathbf{q}}{pRT}\cdot\mathbf{c}\Big(\frac{\mathbf{c}^2}{5RT}-1\Big)\Big). \tag{5.7}$$

Since the quantities, such as the stress and the heat flux, are invariants for Galilean transformation, we consider the situation when $\mathbf{U}=0$. When $(\mathbf{P}-p\mathbf{I})/(2pRT)$ and $\mathbf{q}/(pRT)$ are much less than 1, namely, in continuum regime, by substituting Eq. (5.7) into collision integral (Eq. (5.2)), the above distribution function gives

$$\Delta[\mathbf{uu}]=-(n/m)\sigma_{ref}c_{r,ref}^{2v}\frac{8}{15\sqrt{\pi}}4^{-v}(RT)^{\frac{1}{2}-v}\Gamma(4-v)\mathbf{p}, \tag{5.8a}$$

$$\Delta\Big[\frac{1}{2}\mathbf{uu^2}\Big]=-(n/m)\sigma_{ref}c_{r,ref}^{2v}\frac{8}{15\sqrt{\pi}}4^{-v}(RT)^{\frac{1}{2}-v}\Gamma(4-v)\frac{2}{3}\mathbf{q}, \tag{5.8b}$$

where Γ denotes the Gamma function. The viscosity of the VHS molecule and the mean collision rate $(1/\tau)$ per molecule in an equilibrium gas of VHS molecules are given by the reference [21]. Here we reformulate them as following,

$$\mu=\frac{15m\sqrt{\pi}4^v(RT)^{\frac{1}{2}+v}}{8\Gamma(4-v)\sigma_{ref}c_{r,ref}^{2v}}, \tag{5.9a}$$

$$\frac{1}{\tau}=4nc_{r,ref}^{2v}\sigma_{ref}4^{-v}(RT)^{\frac{1}{2}-v}\Gamma(2-v)/\sqrt{\pi}. \tag{5.9b}$$

Using the above results, the relaxation process of moments of the Boltzamnn equation can be written as,

$$\frac{\partial nf}{\partial t}=-\frac{1}{\tau}(nf-(\tau\mathcal{J}(nf)+nf)),\quad \frac{\partial p_{ij}}{\partial t}=-\frac{p}{\mu}p_{ij},\quad \frac{\partial q_i}{\partial t}=-\frac{2}{3}\frac{p}{\mu}q_i. \tag{5.10}$$

Actually, for VHS molecule in a local equilibrium state, the C_{es} can be derived as [21],

$$\frac{1}{\tau}=\frac{30}{(7-2\omega)(5-2\omega)}\frac{p}{\mu},\quad C_{es}=1-\frac{(7-2\omega)(5-2\omega)}{30}. \tag{5.11}$$

Here C_{es} is confined in a domain of $[0.2,0.5]$ for VHS molecules and can be taken as a constant. For the force driven Poiseuille flow and unsteady boundary heating problem, when C_{es} is in such range, the generalized kinetic model presents better results. But when the Knudsen number changes, the optimized C_{es} also changes. We attribute this kind of observation to the nature of Boltzmann equation.

Hereafter we consider another kind of distribution function and show that C_{es} is highly dependent on the specific form of distribution function. Assume the distribution function is composed of two delta function, say,

$$f=\alpha\delta(\mathbf{u}-(1-\alpha)\mathbf{u}_0)+(1-\alpha)\delta(\mathbf{u}+\alpha\mathbf{u}_0), \tag{5.12}$$

where $\mathbf{u}_0=(u_0,0,0)$ and $\alpha\in[0,1]$, u denotes molecule velocity in x direction. Then the pressure, stress tensor and heat flux can be expressed by α and u_0,

$$p=\frac{1}{3}mn\alpha(1-\alpha)u_0^2,\quad P_{11}=3p,\quad q_1=\frac{1}{2}mn\alpha(1-\alpha)(1-2\alpha)u_0^3. \tag{5.13}$$

The collision rate is

$$\frac{1}{\tau}=2n\pi d_{ref}^2c_{r,ref}^{2v}\alpha(1-\alpha)u_0^{1-2v},\qquad 0\le v<1/2, \tag{5.14a}$$

$$\frac{1}{\tau}=n\pi d_{ref}^2c_{r,ref},\qquad v=1/2. \tag{5.14b}$$

Note that the $1/\tau$ is not continuous when $v=1/2$, because the collision cross section between two molecules with identical velocity is infinite when $v=1/2$. It is inappropriate to count this kind of collision. So we will discuss the case of $0\le v<1/2$. Substituting Eq. (5.12) into Eq. (5.2), the collision terms give,

$$m\Delta[u^2]=-\frac{1}{\tau}p_{11}\frac{(q_1/\rho)^2+(P_{11}/\rho)^3}{(P_{11}/\rho)^3},\quad m\Delta\left[\frac{1}{2}u\mathbf{u}^2\right]=-\frac{1}{\tau}\frac{2}{3}q_1\frac{(q_1/\rho)^2+(P_{11}/\rho)^3}{(P_{11}/\rho)^3}. \tag{5.15}$$

Here, the relaxation process is totally different from the near equilibrium state as shown before. C_{es} in this case can be formally written as

$$C_{es}=1-\frac{(q_1/\rho)^2+(P_{11}/\rho)^3}{(P_{11}/\rho)^3}.$$

Obviously, it is not a constant. Furthermore, it is less than 0 and can even go to minus infinity. The situation described here always happens in near free molecular flow, especially for the case where spatial variation is large. As an example in the one dimensional case, the solution of free molecular flow is,

$$f(x,u,t)=f_0(x-ut,u,t),\quad \frac{\partial f}{\partial u}=-t\frac{\partial f_0}{\partial x}+\frac{\partial f_0}{\partial u}.$$

If the initial condition is nonuniform, discontinuous distribution function will emerge.

For boundary temperature variation problem, the value of C_{es} is preferred to recover the ES-model, namely, $C_{es}=-0.5$. The Fig. 8 shows the distribution function at $(0,0.5)$. Based on the above analysis, two peak structure corresponds to a negative value of C_{es}. Therefore, we qualitatively conclude that the ES-model is more appropriate for this problem.

As show above, C_{es} is not a constant due to the nature of the Boltzmann equation. Even with distribution function Eq. (5.7), C_{es} is nonconstant if high order terms are taken into consideration. With such understanding, we construct a variable C_{es} in the shock structure calculation in order to get a good agreement with DSMC. As show in Fig. 9, a

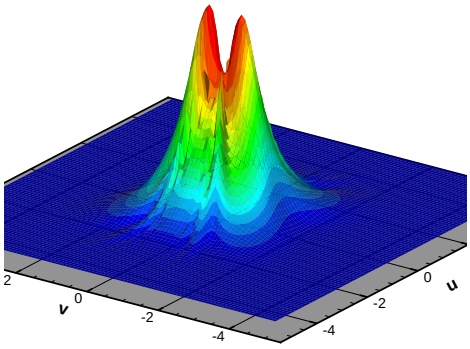

Figure 8: The distribution function at location $(0,0.5)$ for spatially varying boundary temperature heating problem.

good shock structure can be obtained and the corresponding C_{es} is plotted for this calculation. The stress is normalized by $\rho_1 RT_1$ and the heat flux is normalized by $\rho_1(RT_1)^{3/2}$. The temperature, stress and heat flux profile are improved a lot, while the density profile changes only a little bit. The early raising of temperature profile in the upstream is suppressed efficiently. In the past years, some similar kinetic models [5, 26] have been proposed. But people always try to find a universal optimized parameter which might not exist under current framework of kinetic models. Variables or functional instead of a fixed parameter might be more suitable for kinetic models. Based on these numerical results and analysis, we believe that the new free parameter in the generalized kinetic model has significant physical insight which deserves its further study.

Owing to the existence of negative C_{es}, the ES-model might be incapable for such simulation, since the ES-model always constrains C_{es} in the interval $[-0.5,1)$ to keep a positive eigenvalue of $\mathbf{T}$. Here, an alternative of Gaussian distribution can be adopted in the kinetic model,

$$\mathcal{G}[f]\approx\mathcal{M}[f](1+\mathbf{c}\cdot\mathbf{T}'\cdot\mathbf{c}), \tag{5.16}$$

where

$$T'_{ij}=\frac{1}{2(RT)^2}T_{ij},\quad i\neq j, \tag{5.17}$$

and

$$T'_{ij}=\frac{1}{2(RT)^2}(T_{ij}-\text{trace}(\mathbf{T})/3),\quad i=j. \tag{5.18}$$

The lower bound of C_{es} for Gaussian distribution can be removed. Surprisingly, although the above expansion cannot guarantee the positivity of the distribution function, the numerical results from the above expansion are very close to that where a full Gaussian distribution function is used. The increase of the computational cost of the combined the the ES-model and S-model is only about 15% compared with the S-model. If the expansion of ES-model is used, the coefficients of different models can be merged before calculation. So the computational cost is almost identical to that for S-model.

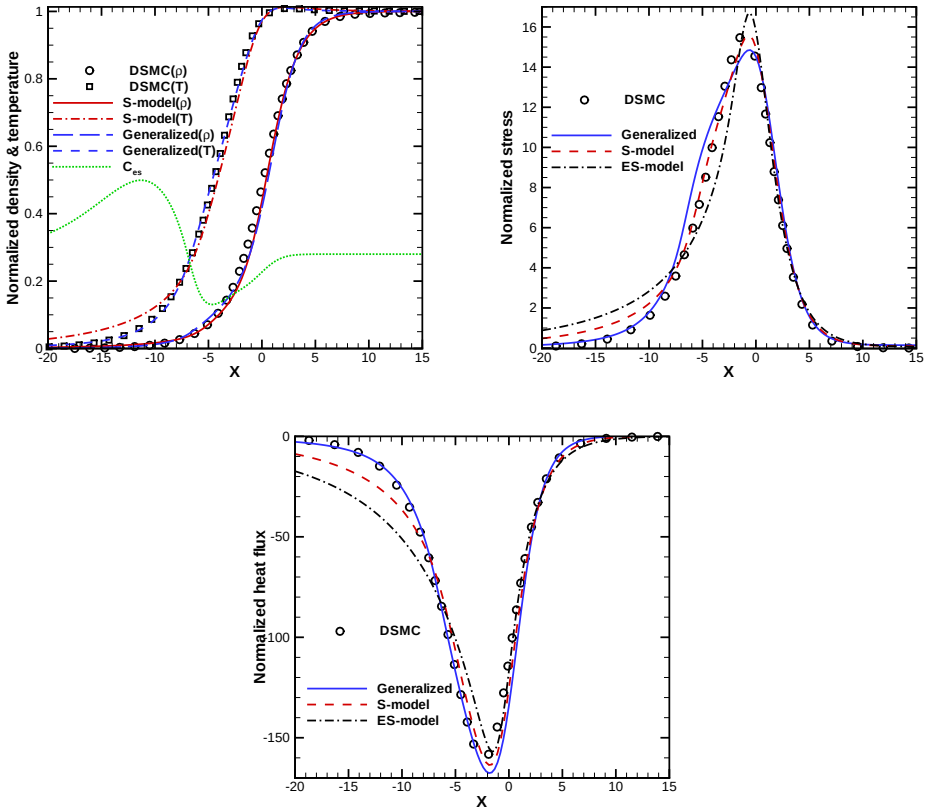

Figure 9: The shock structure from the generalized kinetic model with a variable C_{es} at Ma$=8$ and $\omega=0.81$.

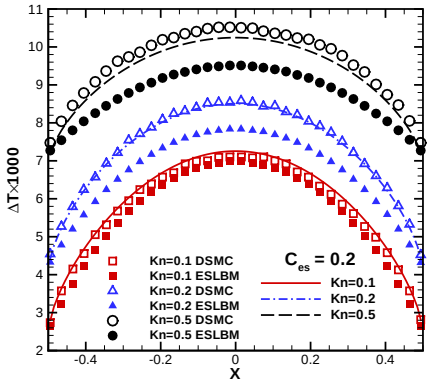

Figure 10: Comparison of the temperature profiles for low speed Couette flow problem. The DSMC and ESLBM results are extracted from the reference by [22].

6 Conclusions

In this paper, we have developed a generalized kinetic model through the combination of the ES-model and the S-model. With a fixed Prandtl number, this new model pro-

vides an additional free parameter, which can be used to cope with the complicated non-equilibrium flow physics and recover the physical solution more accurately. By adjusting the free parameter, different relaxation times between different moments of a gas distribution function can be simulated. With the variation of this free parameter, the new model covers the BGK model, ES-model and Shakhov model. Meanwhile, it provides a continuum spectrum of kinetic models with different dynamics.

The numerical study and analysis indicates that, due to the relaxation of Boltzmann collision term (Eqs. (5.8) and (5.15)), an important property for a kinetic model to capture physically valid solutions is the ratios between the relaxation rates of different moments of a gas distribution function. In most cases, the S-model presents reasonable numerical results. In the near continuum regime, parameters deduced from linear problem is recommended, such as Eq. (5.11). In transition regime, the optimized parameter is larger than 0 when isothermal boundary condition is applied, or less than 0 when large temperature gradients exist in the boundary. As shown in Fig. 10, the generalized model can present accurate results, especially for low speed and weakly non-equilibrium problems.

We believe that the kinetic models presented in this paper, along with the unified scheme, will be very useful for the microflow studies in vacuum industry.

Acknowledgments

We would like to thank Yonghao Zhang and Lei Wu for their helpful comments and suggestions. This work was supported by Hong Kong Research Grant Council (621011, 620813) and SRFI11SC05 at HKUST and the National Natural Science Funds for Distinguished Young Scholar group under Grant No. 11221061.

References

[1] P. L. BHATNAGAR, E. P. GROSS AND M. KROOK, *A model for collision processes in gases*, Phys. Rev., 94 (1954), pp. 511–525.
[2] L. H. HOLWAY, *New statistical models for kinetic theory: Methods of construction*, Phys. Fluids, 9(9) (1966), pp. 1658–1673.
[3] P. ANDRIES AND B. PERTHAME, *The ES-BGK model equation with correct Prandtl number*, AIP Conf. Proc., 585 (2001), pp. 30–36.
[4] E. M. SHAKHOV, *Generalization of the Krook kinetic relaxation equation*, Fluid Dynamics, 3 (1968), pp. 95–96.
[5] G. LIU, *A method for constructing a model form for the Boltzmann equation*, Phys. Fluids A, 2 (1990), 277.
[6] P. ANDRIES, J. BOURGAT, P. LE TALLEC AND B. PERTHAME, *Numerical comparison between the Boltzmann and ES-BGK model for rarefied gases*, Comput. Methods Appl. Mech. Eng., 191 (2002), pp. 3369–3390.
[7] V. GARZÓ, M. DE HARO AND M. LÓPEZ, *Kinetic model for heat and momentum transport*, Phys. Fluids, 6 (1994), 3787.

[8] I. A. GRAUR AND A. P. POLIKARPOV, *Comparison of different kinetic models for the heat transfer problem*, Heat Mass Transfer, 46 (2009), pp. 237–244.
[9] Y. ZHENG AND H. STRUCHTRUP, *Ellipsoidal statistical Bhatnagar-Gross-Krook model with velocity-dependent collision frequency*, Phys. Fluids, 17 (2005), 127103.
[10] A. N. KUDRYAVTSEV, A. A. SHERSHNEV AND M. S. IVANOV, *Comparison of different kinetic and continuum models applied to the shock-wave structure problem*, AIP Conf. Proc., 1084 (2008), pp. 507–512.
[11] L. MIEUSSENS, *Numerical comparison of Bhatnagar-Gross-Krook models with proper prandtl number*, Phys. Fluids, 16 (2004), 2797.
[12] K. XU AND JUAN-CHEN HUANG, *A unified gas-kinetic scheme for continuum and rarefied flows*, J. Comput. Phys., 229 (2010), pp. 7747–7764.
[13] KUN XU AND JUAN-CHEN HUANG, *An improved unified gas-kinetic scheme and the study of shock structures*, IMA J. Appl. Math., 76 (2011), pp. 698–711.
[14] J. C. HUANG, K. XU AND P. B. YU, *A unified gas-kinetic scheme for continuum and rarefied flows ii: Multi-dimensional cases*, Commun. Comput. Phys., 12 (2012), pp. 662–690.
[15] J. C. HUANG, K. XU AND P. B. YU, *A unified gas-kinetic scheme for continuum and rarefied flows iii: Microflow simulations*, Commun. Comput. Phys., 14 (2011), pp. 1147–1173.
[16] S. Z. CHEN, K. XU, C. B. LEE AND Q. D. CAI, *A unified gas kinetic scheme with moving mesh and velocity space adaptation*, J. Comput. Phys., 231 (2012), pp. 6643–6664.
[17] H. GRAD, *On the kinetic theory of rarefied gases*, Commun. Pure Appl. Math., 2 (1949), pp. 331–407.
[18] H. STRUCHTRUP AND M. TORRILHON, *Regularization of grad's 13 moment equations: Derivation and linear analysis*, Phys. Fluids, 15 (2003), 2668.
[19] K. XU, *A gas-kinetic BGK scheme for the Navier-Stokes equations and its connection with artificial dissipation and godunov method*, J. Comput. Phys., 171 (2001), pp. 289–335.
[20] J. MENG, Y. ZHANG, AND J. M. REESE, *Assessment of the ellipsoidal-statistical Bhatnagar-Gross-Krook model for force-driven poiseuille flows*, J. Comput. Phys., 251 (2013), pp. 383–395.
[21] G. A. BIRD, Molecular Gas Dynamics and the Direct Simulation of Gas Flows, Clarendon Press, Oxford, 1994.
[22] J. MENG, Y. ZHANG, N. G. HADJICONSTANTINOU, G. A. RADTKE AND X. SHAN, *Lattice ellipsoidal statistical BGK model for thermal non-equilibrium flows*, J. Fluid Mech., 718 (2013), pp. 347–370.
[23] T. M. M. HOMOLLE AND N. G. HADJICONSTANTINOU, *Low-variance deviational simulation Monte Carlo*, Phys. Fluids, 19 (2007), 041701.
[24] G. A. RADTKE, N. G. HADJICONSTANTINOU AND W. WAGNER, *Low-noise Monte Carlo simulation of the variable hard sphere gas*, Phys. Fluids, 23 (2011), 030606.
[25] S. HARRIS, An Introduction to the Theory of the Boltzmann Equation, Dover Publications, Inc, 2004.
[26] V. I. ZHUK, V. A. RYKOV AND E. M. SHAKHOV, *Kinetic models and the shock structure problem*, Fluid Dynamics, 8 (1973), pp. 620–625.